

Quasi-stationary states in low-dimensional Hamiltonian systems

Fulvio Baldovin, Edgardo Brigatti and Constantino Tsallis
 Centro Brasileiro de Pesquisas Físicas
 Rua Xavier Sigaud 150, 22290-180 Rio de Janeiro-RJ, Brazil

We connect results of Hamiltonian nonlinear dynamical theory with thermodynamics. Using a properly defined dynamical temperature in low-dimensional symplectic maps, we display and characterize long-standing quasi-stationary states that eventually cross over to a Boltzmann-Gibbs-like regime. As time evolves, the geometrical properties (e.g., fractal dimension) of the phase space change dramatically, and the duration of the anomalous regime diverges with decreasing chaoticity. The scenario that emerges is consistent with the nonextensive statistical mechanics one.

PACS numbers: 05.10.-a, 05.20.Gc, 05.45.Ac, 05.60.Cd.

The foundation of the Boltzmann-Gibbs (BG) equilibrium thermodynamics lies on a sufficiently complete and uniform occupation of the system phase space, taking into account symmetry, energy and similar restrictions. However, as a consequence of the rapidly boosting interest in complex systems, physical situations that do not fulfill this condition are nowadays becoming a central topic, and there are already many evidences of dynamical and thermodynamic anomalies in systems like turbulent fluids [1], high-energy collision processes [2], classical and quantum chaos [3], economics [4], motion of micro-organisms [5], and others. One of these anomalies, recently observed in many-body long-range-interacting Hamiltonian systems, is the emergence of long-standing quasi-stationary (metastable) states (QSS) characterized by non-Gaussian velocity distributions, before the BG equilibrium is attained [6,7]. In this letter we point out previously unexposed connections between nonlinear chaos theory and thermodynamics. We observe in fact that the Kolmogorov-Arnold-Moser (KAM) theory provides a background for the explanation of anomalous states similar to those described in [6,7] (and references therein), and, using low-dimensional symplectic maps, we exhibit QSS and study their fundamental features.

If one considers the phase space (\mathbb{R}^n) of the system, the BG equilibrium descends from the equal-a-priori-probability postulate, that characterizes the micro-canonical Gibbsian ensemble (see, e.g., [8]). According to this postulate, each equally-sized accessible region of the phase space (under the macroscopic conditions of the system) equally likely contains the microscopic state of the system. As Einstein pointed out in his criticism of the Boltzmann principle $S = k \ln W$ [9], only the underlying dynamics of the system can justify such postulate. Indeed, if the system is sufficiently chaotic, the postulate is a very accurate representation of the dynamical behavior, as testifies more than a century of successes of the BG formalism. But what about those situations where the system displays weak chaos, like at the border between regularity and chaoticity?

At this border, for a large class of Hamiltonian systems, a mechanism based on the KAM theory operates, which we briefly review now. A continuous Hamiltonian system with n degrees of freedom may be written in the form:

$$H = H_0(I_1; \dots; I_n) + V(I_1; \dots; I_n; \dot{I}_n); \quad (1)$$

where H_0 is integrable ($I_1; \dots; I_n$ are its integrals of motion), $\ll 1$, and V is a nonlinear perturbation. Under certain hypothesis (see, e.g., [10]), for $\epsilon = 0$ the trajectories lie on invariant n -dimensional tori. A special subset of these tori are called resonance tori. Specifically, if we introduce the (non-degenerate) frequencies of the unperturbed motion: $\omega_j = \frac{\partial H_0}{\partial I_j}$ ($j = 1; \dots; n$), we have that the condition $\sum_{j=1}^n m_j \omega_j = 0$ (where m_j are integer numbers) defines the resonance tori. Each resonance torus involves the formation of a separatrix loop. The action of the perturbation, for small enough $\epsilon \neq 0$, deforms normal tori into KAM-tori, and, in correspondence with the resonance tori, destroys the separatrices replacing them with stochastic layers. Resonance tori, in the space spanned by $I_1; \dots; I_n$, lie in the intersection between the hyperplane defined by the resonance condition and the hypersurface of energy $E = H_0(I_1; \dots; I_n)$. In the case $n > 2$, resonance tori must, for topological reasons, intersect between them. Consequently, while for $n = 2$ the stochastic layers are distinct for sufficiently small, for $n > 2$ they merge into a single connected stochastic web that is dense in the phase space for all $\epsilon \neq 0$, and there is room for A-mold diffusion processes. We remark that KAM-tori constitute total barriers for diffusive processes in the phase space; nevertheless, inside the stochastic sea, it is possible to find Cantor sets, named cantori, that constitute partial barriers for diffusion (see [11] for details).

A convenient way of studying Hamiltonian systems is by using symplectic maps. A $(2n-2)$ -dimensional symplectic map is obtained from conservative Hamiltonian systems with n degrees of freedom by taking a Poincaré

section over the hypersurface of constant energy (alternatively, a $(2n-1)$ -dimensional symplectic map is also the result of a Poincaré section on the phase space of a system of n degrees of freedom with a Hamiltonian that depends periodically on time). The advantage of maps lies on the reduced dimension of the phase space and on the use of a discrete time. Let us start through the analysis of a prototypical 2-dimensional symplectic map ($n=2$), the standard (or kicked rotor) map

$$\begin{aligned} p(t+1) &= p(t) + \frac{a}{2} \sin[2\pi p(t)] + \alpha(t) \pmod{1}; \\ p(t+1) &= p(t) + \frac{a}{2} \sin[2\pi p(t)] \pmod{1} \end{aligned} \quad (2)$$

($a \in \mathbb{R}$; $t = 0; 1; \dots$); p may in fact be regarded as the angular momentum of a free rotor subject to angle-dependent impulses of strength a at unit intervals of time. Notice that in order to have an upper bound in p^2 , we have used the symmetry properties of the map and defined the angular momentum $p \pmod{1}$. The standard map is integrable for $a = 0$, while chaoticity rapidly increases with $|a|$.

In [6,7], the emergence of the dynamical QSS appeared to be dependent on the initial conditions. Specifically, it was shown that for some classical long-range-interacting N-rotor Hamiltonian models, a basin of attraction of initial data exist for which the system dynamically evolves into a QSS whose duration diverges as $N \rightarrow \infty$. Typical examples of this basin of attraction are the so called 'Water bag' initial conditions, characterized by a uniform initial distribution of the angular momenta around zero. Coming back to the standard map, we first observe that the points $(0;1=2)$ and $(1=2;1=2)$ are a 2-cycle for all a . A 'back bone' of elliptic-hyperbolic points always passes through them and they constitute then a good referential for studying the properties of the phase space with respect to variation of the parameters. In order to simulate 'Water bag' initial conditions in the angular momentum we consider at $t = 0$ a statistical ensemble of M copies of the standard map with arbitrary p and p randomly distributed in a small region around $p = 1/2$. In analogy with [6,7] we can then define the (dimensionless) 'dynamical temperature' of the ensemble as the variance of the angular momentum: $T = \langle p^2 \rangle - \langle p \rangle^2$, where $\langle \cdot \rangle$ means ensemble average. The temperature associated to the uniform ensemble (that we will call BG temperature) is given by $T_{BG} = \frac{1}{2} \int_0^{R_1} dp p^2 = 1/12$.

For large values of $|a|$ (i.e., strong chaoticity) in map (2), the temperature of the 'Water bag' initial ensemble rapidly relaxes to T_{BG} . Our aim is to study what happens in the transition to regularity obtained reducing the value of $|a|$ towards $a = 0$. In Fig. 1(a) we see that the first effect of the reduction of $|a|$ is that $\lim_{t \rightarrow \infty} T(t) < T_{BG}$. This is easily understood as follows. As chaoticity reduces, total barriers (KAM-tori) appear in the phase space. As a consequence, the points of the ensemble are prevented to reach all the regions of

the phase space and the projection of the ensemble on the p axis produces a probability distribution function (PDF) with a variance smaller than the one of the uniform distribution. For values of a of order $a \approx 1$, a QSS emerges before the relaxation to the natural temperature. In fact, inside the stochastic sea partial barriers (cantori) begins to appear, and the initial 'water bag' first rapidly diffuse inside an area delimited by cantori and then slowly crosses over to the natural relaxation temperature. Fig. 1(b) illustrates this behavior. To obtain a quantitative description of the relaxation time we have decided to plot the iteration time in a logarithmic scale. We define the crossover time t_c as the injection point of the curve and we observe that it diverges, as a tends to $a_c = 0.971635406 \dots$ from above, like $t_c \sim (a - a_c)^{2/7}$ (see inset of Fig. 1(a)). Just below this critical value in fact, the strongest cantori close [11], and the relaxation to a higher temperature is prevented. Reducing a to smaller values causes the formation of more and more total barriers, so that the 'dynamical temperature' tends to zero for $|a| < 0$. From the mechanism we have displayed, it is clear that it is possible to obtain these types of QSS even with other sets of initial conditions. Typically, it is sufficient to have the initial data localized inside the first partial barriers. In other words there is an entire basin of attraction of far from equilibrium initial conditions that leads to the formation of a certain kind of QSS.

As we pointed out previously, the topology of the phase space changes dramatically for $n > 2$. To address this case, we move next to a 4-dimensional symplectic map composed by two coupled standard maps:

$$\begin{aligned} p_1(t+1) &= p_1(t) + \frac{a_1}{2} \sin[2\pi p_1(t)] + \alpha_1(t) + b p_2(t); \\ p_1(t+1) &= p_1(t) + \frac{a_1}{2} \sin[2\pi p_1(t)]; \\ p_2(t+1) &= p_2(t) + \frac{a_2}{2} \sin[2\pi p_2(t)] + \alpha_2(t) + b p_1(t); \\ p_2(t+1) &= p_2(t) + \frac{a_2}{2} \sin[2\pi p_2(t)]; \end{aligned} \quad (3)$$

where $a_1, a_2, b \in \mathbb{R}$; $t = 0; 1; \dots$, and all variables are defined $p \pmod{1}$. If the coupling constant b vanishes the two standard maps decouple; if $b = 0$ the points $(0;1=2;0;1=2)$ and $(1=2;1=2;1=2;1=2)$ are a 2-cycle for all (a_1, a_2) , hence we preserve, in phase space the same referential that we had for a single standard map. For a generic value of b , all relevant present results remain qualitatively the same. Also, we set $a_1 = a_2 = a$ so that the system is invariant under permutation $1 \leftrightarrow 2$. Since we have two rotors now, the 'dynamical temperature' is naturally given by $T = \frac{1}{2} \langle p_1^2 \rangle + \langle p_2^2 \rangle - \langle p_1 \rangle^2 - \langle p_2 \rangle^2$, hence the BG temperature remains $T_{BG} = 1/12$.

As before we consider 'Water bag' initial conditions, i.e., an ensemble of M points with arbitrary (p_1, p_2) , and angular momenta randomly distributed inside a small region around $p_1 = p_2 = 1/2$. The result is qualitatively similar to the one displayed in Fig. 1(a) for $a > a_c$. Large

values of α correspond to T_{BG} and reducing α we observe the formation of a Q SS that, after some time, relaxes to a temperature $T < T_{BG}$. The first major difference with the 2-dimensional case is that, because of the A model diffusion processes, the relaxation to a higher temperature occurs (waiting enough time) for all $\alpha \neq 0$ (i.e., $\alpha_c = 0$, defining α_c as the value where t_c diverges). Moreover, the reason why the ensemble does not relax to the BG temperature for small values of α is here quite different from that for the 2-dimensional case. Indeed, with this choice of initial data, the initial 'water bag' intersects at least a macroscopic island, as clearly appreciated in Fig. 2 (a1); the points that are set inside the island do not diffuse to the outside. As a result, the projection of the ensemble on the plane $p_1; p_2$ conserve a denser central part for all times (Fig. 2 (b1), (c1)).

If we instead shift the initial 'water bag', say towards the lower part of the phase space, we can set the points outside this island (Fig. 2 (a2)–(c2)). In this case we obtain a crucial qualitatively new phenomenon, namely the formation, for small values of α , of a Q SS that eventually relaxes to the BG temperature (see Fig. 3(a)). Notice also that the crossover time t_c diverges, as $\alpha \rightarrow 0$, faster than in the 2-dimensional case: $t_c \sim 1/\alpha^{5/2}$ (see inset of Fig. 3(a)). We remark that the relaxation to the BG temperature occurs here even if the presence of islands in the phase space violate the *equal a priori* postulate. In other words, it is possible to obtain a weak violation of the postulate that does preserve a uniform distribution once the ensemble is projected over the plane $p_1; p_2$, in the same sense that a sponge projects a uniform shadow on a wall. These Q SS can in fact be geometrically characterized by the fractal dimension d_f . Overcoming some numerical difficulties involved in a fractal analysis in 4 dimensions, we illustrate what happens in Fig. 3(b), constructed using a box-counting algorithm [12] (in fact, the phase space exhibits strong inhomogeneities which suggest a multifractal structure). During the Q SS the ensemble is, for small α , associated with a nontrivial fractal dimension $d_f \approx 2.7$, while, once it crosses over to the BG-like regime, it distributes itself occupying the full dimensionality of the phase space, thus attaining $d_f = 4$.

The simplicity of the present models allow us also for the discussion of different types of Q SS. For instance, at $t = 0$ we can set up 'double waterbag' initial conditions considering an ensemble of M copies of two coupled standard maps with arbitrary $p_1; p_2$ and angular momenta randomly distributed inside two small regions: $p_1; p_2 = 0+$ and $p_1; p_2 = 1$ ($0 < < 1$). In this case, the initial temperature $T(0)$ is higher than T_{BG} , because the PDFs projected on the $p_1; p_2$ axes are double peaked. Relaxation to T_{BG} occurs then from above, as can be seen in Fig. 4. This is precisely in what the phenomenon observed in [7,13] differs from the one in [6].

Through the numerical analysis of low-dimensional symplectic maps, we have shown how the complex and rich structures associated with conservative nonlinear dynamics can generate anomalous thermodynamical behav-

ior. Particularly, we have exhibited and studied the emergence, while approaching integrability (i.e., when chaoticity decreases), of Q SS suggestively similar to those observed in long-range N-body systems (a playing a role analogous to $1=N$). A central result is that, in contrast with what happens for the BG equilibrium, these Q SS correspond to a nontrivial fractal dimension. This observation is consistent with the scenario where nonextensive statistical mechanics [14] seems to apply.

ACKNOWLEDGMENTS

We thank C. Anteneodo, A. K. Ringer, A. Rapisarda, A. Robledo and J. de Souza for useful remarks, as well as CAPES, PRONEX, CNPq and FAPERJ (Brazilian agencies) for partial support.

- [1] C. Beck, G.S. Lewis and H.L. Swinney, *Phys. Rev. E* **63**, 035303 (2001); C. Beck, *Phys. Rev. Lett.* **87**, 180601 (2001); T. Arimitsu and N. Arimitsu, *Physica A* **305**, 218 (2002).
- [2] I. Bediaga, E.M.F. Curado and J.M. Iranda, *Physica A* **286**, 156 (2000); C. Beck, *Physica A* **286**, 164 (2000).
- [3] Y.S. Weinstein, S. Lloyd and C.T. Sallis, *Phys. Rev. Lett.* **89**, 214101 (2002); E.P. Borges, C.T. Sallis, G.F.J. Ananos and P.M. C. Oliveira, *Phys. Rev. Lett.* **89**, 254103 (2002).
- [4] L. Boland, *Phys. Rev. Lett.* **89**, 098701 (2002).
- [5] A. Upadhyaya, J.-P. Rieu, J.A. G. Lazier and Y. Sawada, *Physica A* **293**, 549 (2001).
- [6] V. Latora, A. Rapisarda and C.T. Sallis, *Phys. Rev. E* **64**, 056134 (2001); A. Campa, A. Giansanti and D. M. Ortoni, *Physica A* **305**, 137 (2002); B. J.C. Cabral and C.T. Sallis, *Phys. Rev. E* **66**, 065101(R) (2002); M. A. M. Ontemuro, C. Anteneodo and F. Tamari, *Phys. Rev. E* (2003), in press.
- [7] F.D. Nobre and C.T. Sallis, cond-mat/0301492.
- [8] K. Huang, *Statistical Mechanics* (J. Wiley and Sons, New York, 1987).
- [9] See, e.g., E.G.D. Cohen, *Physica A* **305**, 19 (2002), and references therein.
- [10] G.M. Zaslavsky, R.Z. Sagdeev, D.A. Ulikov and A.A. Chernikov, *Weak chaos and quasi-regular patterns* (Cambridge University Press, Cambridge 1991).
- [11] R.S. Mackay, J.D.M. Weiss and I.C. Percival, *Physica D* **13**, 55 (1984).
- [12] A.K. Ringer, *Computer Physics Communications*, **98**, 224 (1996).
- [13] E. Borges, private communication.
- [14] C.T. Sallis, *J. Stat. Phys.* **52**, 479 (1988); E.M.F. Curado and C.T. Sallis, *J. Phys. A* **24**, L69 (1991) [Corrigenda: **24**, 3187 (1991) and **25**, 1019 (1992)]. For recent reviews see C.T. Sallis, A.R. Rapisarda, V. Latora and F. Baldovin, in *Dynamics and Thermodynamics of Systems*

with Long-Range Interactions, eds. T. Dauxois, S. Ruffo, E. Amorim and M. W. Hennings, Lecture Notes in Physics 602, 140 (Springer, Berlin, 2002), and M. Gellman and C. T. Sallis, eds., Nonextensive Entropy - Interdisciplinary Applications (Oxford University Press, 2003), in preparation. See <http://tsallis.cat.cbpf.br/biblio.htm> for full bibliography.

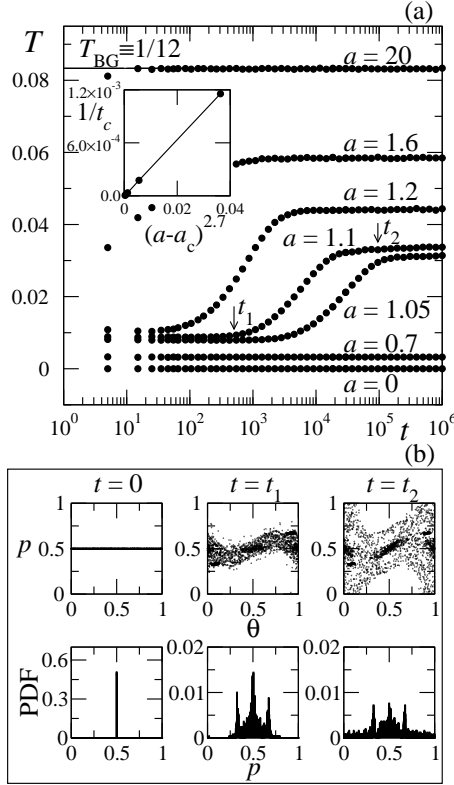


FIG. 1. (a) Time evolution of the dynamical temperature T of a standard map, for typical values of a . We start with 'water bag' initial conditions ($M = 2500$ points in $0 \leq \theta \leq 1$, $p = 0.5 \pm 5 \cdot 10^{-4}$). In order to eliminate cyclical fluctuations, the dots represent average of 10 iteration steps; moreover, each curve is the average of 50 realizations. Inset: Inverse crossover time t_c (in action point between the QSS and the BG regimes) vs. $1 = (a - a_c)^{2.7}$. No linear points subsist if it is linearly represented. (b) Time evolution of the ensemble in (a) for $a = 1.1$ (first row) and PDF of its angular momentum (second row). $t = 0$: 'water bag' initial conditions; $t = t_1 = 500$: the ensemble is mostly restricted by cantori; $t = t_2 = 10^5$: the ensemble is confined inside KAM tori.

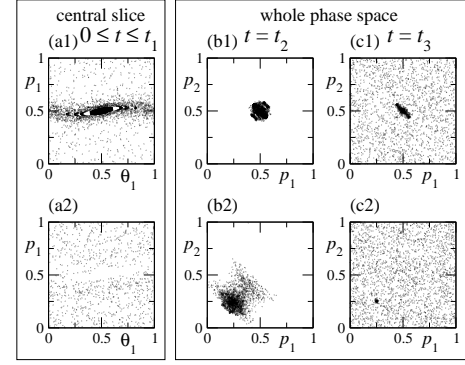


FIG. 2. Phase space analysis of the evolution of 'water bag' ensembles for two coupled standard maps for $(a, b) = (0.4, 2)$. First row: 'water bag' initial conditions $0 \leq \theta_1, 2 \leq 1$, $p_1, p_2 = 0.5 \pm 5 \cdot 10^{-3}$. Second row: 'water bag' initial conditions $0 \leq \theta_1, 2 \leq 1$, $p_1, p_2 = 0.25 \pm 5 \cdot 10^{-3}$. (a) Projection on the (θ_1, p_1) -plane of the central slice of the phase space ($\theta_2, p_2 = 0.5 \pm 10^{-2}$), for the orbit $0 \leq t \leq t_1 = 10^4$. (b), (c) Projection on the (p_1, p_2) -plane of whole phase space for the iterate at time $t_2 = 15$ and $t_3 = 2 \cdot 10^4$.

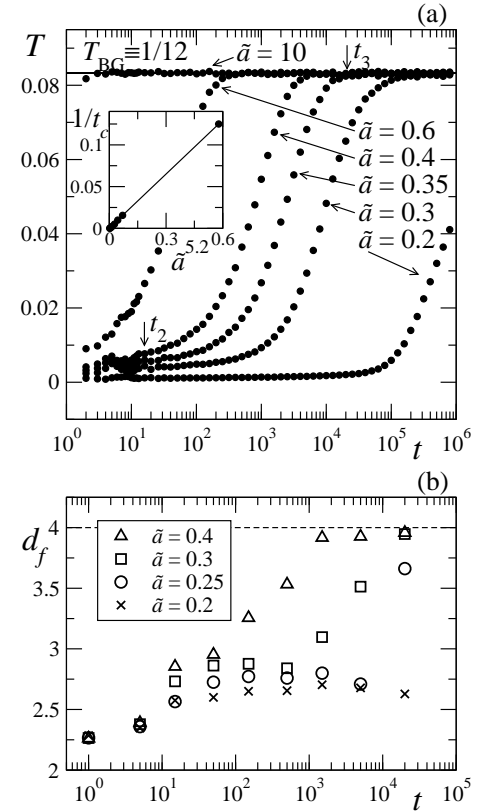


FIG .3. (a) Time evolution of the dynamical temperature T of two coupled standard maps, for $b = 2$ and typical values of α . We start with water bag initial conditions ($M = 1296$ points with $0 \leq p_1, p_2 \leq 1$, and $p_1, p_2 = 0.25 \pm 5 \cdot 10^{-3}$); moreover, an average was taken over 35 realizations. In set: Inverse crossover time t_c vs. $1 = \alpha^{5/2}$. See Fig. 2 for t_2 and t_3 . (b) Time evolution of the fractal dimension of a single initial ensemble in the same setup of (a).

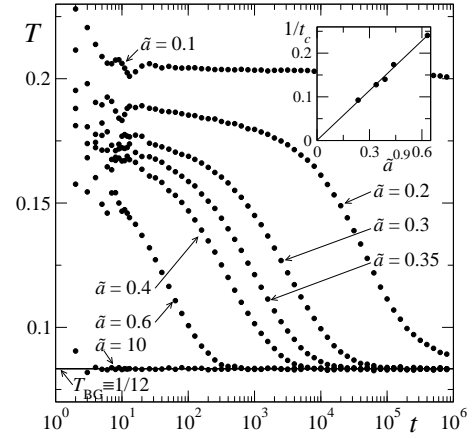


FIG .4. Same as Fig. 3 (a) but with 'double water bag' initial conditions: $0 \leq p_1, p_2 \leq 1$, p_1, p_2 randomly distributed inside one of the two regions $p_1, p_2 = 0 + 10^{-2}$, $p_1, p_2 = 1 - 10^{-2}$.